Distributed Koopman NMPC for Virtually Coupled Train Control

Yiwen Zhang, Lorenzo Calogero, Shukai Li and Anton V. Proskurnikov

***Abstract*— This paper presents a distributed Koopman-based nonlinear model predictive control (NMPC) for virtually coupled train system. Considering nonlinear train dynamics and operational constraints on both states and control inputs, a nonlinear continuous-time tracking control problem is formulated for each train. An analytical observable generation procedure is employed to lift the nonlinear dynamics into the Koopman space, yielding a bilinear lifted system representation. Through bilinearity relaxation and discretization of the lifted dynamics, a linear discrete-time system is obtained, enabling nonlinear programs to be closely approximated by quadratic programs within the MPC framework. Based on a train-to-train communication topology, a distributed implementation is adopted in which each train solves a local optimization problem using updated information received from its preceding train. Simulation results demonstrate that the proposed approach achieves tracking performance comparable to that of a distributed baseline NMPC while significantly reducing computation time, thereby supporting its applicability to real-time virtually coupled train systems.**

I. Introduction

To improve operational efficiency and provide flexible passenger services, virtual coupling has emerged as a promising technology utilizing Train-to-Train (T2T) communication within the next-generation signaling systems [1]. In a virtually coupled train set, a leading train and its subsequent followers move synchronously at short headways using a relative-distance braking mode, thereby enabling high-density operation and improving the utilization of existing lines [2], [3]. However, the relative braking mode, which relies on relative train states, also introduces additional safety concerns. To meet the heightened safety requirements of virtual coupling train control (VCTC), further advances in train control systems are needed to ensure practical applicability.

Several control strategies have been investigated for VCTC systems, including feedback-based, rule-based, heuristic, and optimal-control approaches [4]–[11]. Although these methods improve safety regulation and coordination, they are limited in systematically handling nonlinear dynamics, hard state/input constraints, and online multi-objective optimization under varying operating conditions.

MPC provides a unified framework for handling constraints and tracking objectives in VCTC. Existing MPC-based studies mainly rely on linearized train dynamics and safety constraints [12]–[14]. NMPC improves model fidelity by retaining nonlinear traction, braking, and resistance characteristics [15], [16], but its nonconvex online optimization

Yiwen Zhang and Shukai Li are with the School of Systems Science, Beijing Jiaotong University, China, {yiwenz,shkli}@bjtu.edu.cn

Lorenzo Calogero and Anton V. Proskurnikov are with the Department of Electronics and Telecommunications, Politecnico di Torino, Italy, lorenzo.calogero@polito.it, anton.p.1982@ieee.org

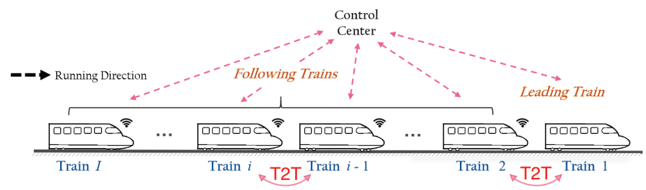

Fig. 1: Diagram of a virtually coupled train formation.

remains computationally demanding for real-time safety-critical implementation.

To overcome the computational challenges of NMPC while retaining modeling fidelity, Koopman operator theory has recently emerged as a promising paradigm for nonlinear control design. The Koopman framework represents nonlinear dynamics as a linear system in a lifted space spanned by observable functions, enabling nonlinear prediction and constraint handling to be carried out in a linear setting. This insight motivates Koopman-based NMPC (KNMPC), lifting the nonlinear prediction model to obtain a linear predictor in the Koopman space and approximating the resulting nonlinear program by a quadratic program with substantially improved computational efficiency [17]–[19].

Recent studies have applied KNMPC to train and vehicle systems, including energy-efficient coordinated control [20]–[23]. However, these works rely on centralized Koopman-based control methods or data-driven Koopman models, which may require large observable sets and suffer from limited generalization and an increased computational burden, particularly when handling safety-critical constraints in virtually coupled train systems. This paper develops a distributed KNMPC framework for the VCTC system based on the information exchanging via T2T communication, using the control strategy from [19]. By combining collision avoidance constraints with an efficient lifted prediction model, the proposed KNMPC framework provides a practical approach for real-time control of virtually coupled trains; we confirm the results by simulations.

II. Problem Setup

We consider a virtual formation consisting of I trains (Fig. 1). Let $i \in \mathcal{I}$ denote the train index, where the train set $\mathcal{I} = \{1, 2, \ldots, I\}$. The first index $i = 1$ denotes the leading train, while the other indexes $i = 2, 3, \ldots, I$ represent the following trains. Information is exchanged among neighboring trains via T2T communication.

A. Train Dynamics and Constraints

According to Newton's laws of kinematics, the differential equations that describe train movements are given by [24]:

$$\begin{cases} \dot{p}_i(t) = v_i, \\ \dot{v}_i(t) = u_i - \left(c_{0i} + c_{1i}v_i + c_{2i}v_i^2\right) - r_i, \\ p_i(t_0) = p_{ini,i}, v_i(t_0) = v_{ini,i}. \end{cases} \tag{1}$$

for all $i \in \mathcal{I}$, where $p_i(t)$ and $v_i(t)$ are position and speed of train i at time instant t, respectively. $u_i(t)$ is control force per unit mass. c_{0i}, c_{1i} and c_{2i} are train-specific coefficients. $r_i(t)$ is the additional resistance per unit mass. Let $x_i(t) = [p_i(t), v_i(t)]^{\mathrm{T}}$ denote the state variable.

The train speed and the control force are constrained as:

$$0 \le v_i(t) \le v_i^{max}(t), \tag{2}$$

$$u_i^{min} \le u_i(t) \le u_i^{max}, \tag{3}$$

where $v_i^{max}(t)$ is the maximum allowable speed. $u_i^{min} < 0$ is the minimum braking force and $u_i^{max} > 0$ is the maximum tractive force. To ensure passenger comfort, the change rate of the control force $\dot{u}_i(t)$ is constrained as:

$$\Delta u_i^{min} \le \dot{u}_i(t) \le \Delta u_i^{max}, \tag{4}$$

where Δu_i^{min} and Δu_i^{max} are lower and upper bounds of $\dot{u}_i(t)$, respectively.

To guarantee safe operation, the collision avoidance constraint for virtually coupled trains is given as:

$$p_{i-1}(t) - p_i(t) - L_{i-1} \ge sm_0, \tag{5}$$

$$p_{i-1}(t) - p_i(t) - L_{i-1} \ge \frac{v_i^2(t)}{2b_{e,i}} - \frac{v_{i-1}^2(t)}{2b_{e,i-1}} + sm_0, \tag{6}$$

where L_{i-1} is the length of train $i-1$. $b_{e,i}$ is emergency braking rate of train i. sm_0 is the minimum safety margin.

B. Objective Function

In a virtually coupled train set, the leading train plays a dominant role in guiding the train set to operate along a reference trajectory, while the following train is responsible for maintaining high-density operation. To achieve coordinated operation, the spacing deviation $\Delta p_i(t)$ and speed deviation $\Delta v_i(t)$ are introduced as:

$$\Delta p_i(t) = \begin{cases} p_{i-1}(t) - p_i(t) - \mathcal{D}_i(t), & \text{if } i = 2, \ldots, I, \\ p_i(t) - p_{ref}(t), & \text{if } i = 1, \end{cases} \tag{7}$$

$$\Delta v_i(t) = \begin{cases} v_i(t) - v_{i-1}(t), & \text{if } i = 2, \ldots, I, \\ v_i(t) - v_{ref}(t), & \text{if } i = 1, \end{cases} \tag{8}$$

where p_{ref} and v_{ref} are the reference position and speed of the leading train, respectively. $\mathcal{D}_i(t)$ denotes the target space interval, defined as $\mathcal{D}_i = L_{i-1} + d_{\mathrm{des}}$, where d_{des} is the desired clear gap between consecutive trains; $\mathcal{D}_i$ is chosen as a constant value in this paper.

To achieve high-accuracy tracking control under the VCTC system, the objective function for each train $i \in \mathcal{I}$ is:

$$\min J_i = \int_{t_0}^{t_f} \left(\delta_{p,i}(\Delta p_i)^2 + \delta_{v,i}(\Delta v_i)^2 + \delta_{u,i}u_i^2\right) dt \tag{9}$$

where $\delta_{p,i}$, $\delta_{v,i}$ and $\delta_{u,i}$ are weight coefficients for penalizing space deviation, speed deviation, and energy consumption, respectively; $[t_0, t_f]$ is the problem horizon.

III. Distributed baseline NMPC Approach

In this section, we present a baseline NMPC controller for the VCTC system, which is implemented in discrete time by discretizing the continuous-time models from Section II. At each sampling time instant, a nonlinear MPC-based optimal control problem is constructed for each virtually coupled train, which can be solved with IPOPT solver [25] to obtain an optimal control sequence. The baseline approach provides a reference in both tracking performance and computational efficiency for evaluating the KNMPC approach.

A. Discretized NMPC formulation

MPC is an effective control method to reduce computational complexity by solving the optimal control problem within the predictive horizon. We use the sampling step $k \in \mathcal{Z}_+ = \{0, 1, 2, \ldots\}$ to discretize the problem horizon $[t_0, t_f]$. Let $[k, k + H_p]$ denote the predictive horizon at each sampling step k, $k \in \mathbb{N}$, where H_p is the length of predictive horizon. At sampling step k, $y_i(k + h|k)$ denotes the prediction of y_i at future step $k+h$ based on information available at step k.

For train dynamics (1), operational constraints (2)-(6), the corresponding reformulations for any time step $k + h$, $h = 0, 1, \ldots, H_p$, at the sampling step k under MPC can be rewritten as:

$$\begin{aligned} x_i(k+h+1|k) = x_i(k+h|k) + & \\ \Delta t \cdot \mathscr{G}_i(x_i(k+h|k), u_i(k+h|k)), & \end{aligned} \tag{10}$$

$$0 \le v_i(k+h|k) \le v_i^{max}(k+h|k), \tag{11}$$

$$u_i^{min} \le u_i(k+h|k) \le u_i^{max}, \tag{12}$$

$$\Delta u_i^{min} \le \frac{u_i(k+h+1|k) - u_i(k+h|k)}{\Delta t} \le \Delta u_i^{max}, \tag{13}$$

$$p_{i-1}(k+h|k) - p_i(k+h|k) - L_{i-1} \ge sm_0, \quad \text{if } i = 2, \ldots, I \tag{14}$$

$$\begin{aligned} p_{i-1}(k+h|k) - p_i(k+h|k) - L_{i-1} \ge sm_0 + & \\ + \frac{v_i^2(k+h|k)}{2b_{e,i}} - \frac{v_{i-1}^2(k+h|k)}{2b_{e,i-1}}, \text{ if } i = 2, \ldots, I & \end{aligned} \tag{15}$$

$$p_i(k|k) = p_{ini,i}(k), v_i(k|k) = v_{ini,i}(k), \tag{16}$$

where Δt is the sampling period. $p_{ini,i}(k)$ and $v_{ini,i}(k)$ are initial train position and speed measured at the sampling step k, respectively.

The finite-horizon objective function for train i at the sampling step k is reformulated as:

$$\begin{aligned} \min J_i^B(k) = \sum\nolimits_{h=0}^{H_p} \big(\delta_{p,i}(\Delta p_i(k+h|k))^2 + & \\ + \delta_{v,i}(\Delta v_i(k+h|k))^2\big) + \sum\nolimits_{h=0}^{H_p-1} \delta_{u,i} u_i^2(k+h|k), & \end{aligned} \tag{17}$$

At each sampling step k, the discrete-time NMPC problem for virtually coupled train i within the predictive horizon is given by the following finite-dimensional nonlinear optimization problem:

$$\begin{aligned} &\min \; J_i^B(k) \\ &\text{s.t. constraints (10)} - (16). \end{aligned} \tag{18}$$

Note that the collision avoidance constraints (14) and (15) are considered for the following trains $i = 2, \ldots, I$ based on the states of their preceding trains.

B. Solution Approach

1) Distributed calculation: According to the T2T communication topology of the virtually coupled train set, a distributed control architecture is adopted where each train solves a local NMPC problem according to the information received from its neighbors, thus reducing communication burden and improving scalability of the VCTC system. The distributed receding-horizon procedure is summarized in Algorithm I; The same information-exchange structure is used for both D-BNMPC and D-KNMPC. Specifically, the leading train $i = 1$ formulates its NMPC problem based on the reference trajectory and its current state measurements. For each following train $i = 2, \ldots, I$, the predicted position and speed trajectories of train $i-1$ are transmitted to train i via T2T communication and treated as known parameters in the objective and collision avoidance constraints over the prediction horizon. Each following train then solves its local NMPC problem based on local measurements and the received trajectory of its preceding train. Via the sequential information propagation and local optimizations, coordinated control of the virtually coupled train set is achieved through distributed calculations.

Algorithm 1: Distributed MPC procedure

Step 1 For $i \in \{1, \ldots, I\}$ do
- **Step 1.1:** If $i = 1$, solve the local MPC problem using the reference trajectory $p_{\text{ref}}(k+h)$, $v_{\text{ref}}(k+h)$.
- **Step 1.2** If $i = 2, \ldots, I$,
  Receive the optimal state trajectories $\mathbf{p}_{i-1}^*(k+h|k)$, $\mathbf{v}_{i-1}^*(k+h|k)$ from its preceding train $i-1$; here $h = 1, \ldots, H_p + 1$.
- **Step 1.3** Solve problem (18) for train i with
  $p_{i-1}(k+h|k) = p_{i-1}^*(k+h|k)$, $v_{i-1}(k+h|k) = v_{i-1}^*(k+h|k)$.
  Find the optimal control input $\mathbf{u}_i^*$, and the state trajectories $\mathbf{p}_i^*$, $\mathbf{v}_i^*$.
- **Step 1.4:** Apply the first input $u_i^*(k|k)$ to train i.
- **Step 1.5** If $i = 1, \ldots, I-1$,
  Transmit $\mathbf{p}_i^*(t_k)$ and $\mathbf{v}_i^*(t_k)$ to its following train $i+1$.

end for

Step 2 Set $k \leftarrow k+1$ and repeat.

2) Numerical Solution: Since the considered problem includes nonlinear train dynamics and nonlinear collision-avoidance constraints, the baseline NMPC is implemented in CasADi [26] and solved by IPOPT [25] rather than by the MATLAB MPC Toolbox, which is primarily intended for linear MPC formulations. CasADi enables efficient problem construction and accurate derivative evaluation, while IPOPT provides a reliable numerical solution for constrained nonlinear optimization. This solver configuration is employed for all trains and at all sampling steps in the baseline NMPC approach, providing a benchmark for tracking performance and computational burden compared with the KNMPC approach developed in Section IV.

3) Closed-loop Realization: The distributed baseline NMPC is implemented in a standard receding-horizon fashion to achieve closed-loop control. At each sampling step k, each train solves its local NMPC problem over the predictive horizon $[k, k+H_p]$ and obtains an optimal control input sequence $\mathbf{u}_i^*(k) = [u_i^*(k|k), \ldots, u_i^*(k+H_p-1|k)]^{\mathrm{T}}$. The control horizon is set to $H_c = 1$, i.e., only the first element of the optimized control sequence $u_i^*(k|k)$ is applied before the problem is solved again at the next sampling step.

IV. Distributed Koopman NMPC Approach

To reduce the computational burden of solving nonlinear optimal control problems, the Koopman operator framework is employed to lift nonlinear train dynamics into a higher-dimensional space in which the system evolution can be approximated by linear dynamics. This section presents the Koopman lifting procedure and the resulting KNMPC formulation for the VCTC system, following the analytical framework in [19]. The D-KNMPC approach uses the distributed architecture in Algorithm I, replacing the problem (18) by the lifted problem formulated below.

A. Basis of Observables and Lifted System

According to Koopman operator theory, the nonlinear train dynamics in (1) can be represented as linear dynamics in a lifted space defined by a set of observable functions. Let $z_i(t) = \phi(x_i(t))$ denote the lifted state vector obtained through the nonlinear mapping $\phi(\cdot)$. To construct the observable basis, the initial set of observables is selected to include the system states and the nonlinear terms appearing in the train dynamics. For the longitudinal dynamics, the nonlinear term mainly arises from the aerodynamic drag v_i^2. Therefore, the initial observable set is chosen as: $\Phi_{in} = \{p_i, v_i, v_i^2\}$.

The corresponding initial vector mapping is $\phi_{\text{in}}(x_i) = [p_i, v_i, v_i^2]^\top$. Following the lifting procedure in [19], an infinite-dimensional observable basis is defined as:

$$\Phi = \Phi_{\text{in}} \cup \{v_i^n\}_{n \geq 3}, \quad |\Phi| = \infty, \tag{19}$$

with the lifting mapping $\phi(x_i) = [\phi_{\text{in}}(x_i)^\top; (v_i^n)_{n\geq 3}]^\top$.

To enhance practical applicability, dimensionality reduction is applied. Specifically, given a maximum polynomial degree $\overline{n} \geq 3$, a truncated basis is constructed as $\Phi = \Phi_{\text{in}} \cup \{v_i^n\}_{3 \leq n \leq \overline{n}}$. The lifted state is then partitioned as:

$$z_i = [z_{x,i}^\top, z_{\sigma,i}, z_{\psi,i}^\top]^\top, \tag{20}$$

where $z_{x,i} = [z_{p,i}, z_{v,i}]^\top$, $z_{p,i} = p_i$, $z_{v,i} = v_i$, $z_{\sigma,i} = v_i^2$, and $z_{\psi,i}$ collects the higher-order observables.

From the train dynamics (1) and the reduced lifted state z_i, the truncated bilinear Koopman system is obtained as:

$$\begin{aligned} \dot{z}_i(t) = \begin{bmatrix} \dot{z}_i{}'(t) \\ \dot{z}_i{}''(t) \end{bmatrix} = A_i z_i(t) + B_0 \begin{bmatrix} u_i(t) \\ r_i(t) \end{bmatrix} + \\ + \begin{bmatrix} B_u z_i, B_r z_i \end{bmatrix} \begin{bmatrix} u_i(t) \\ r_i(t) \end{bmatrix} + F_{\text{res},i}(z_i) + E_i, \end{aligned} \tag{21}$$

where $z_i' = [z_{x,i}^\top, z_{\sigma,i}]^\top$, $z_i'' = z_{\psi,i}$. The partition of z_i is introduced since $\dot{z}_i''$ involves the dynamics of unlifted parts of the system, resulting in nonlinear residual terms. Lifted system matrices A_i, B_u, B_r, $F_{\mathrm{res},i}(z_i)$ and E_i can obtained by differentiating each observable along the dynamics (1). Taking $\bar{n} = 3$ (and $\dim z_i = 4$) as an illustrative example, it can be checked that

$$A_i = \begin{bmatrix} 0 & 1 & 0 & 0 \\ 0 & -c_{1i} & -c_{2i} & 0 \\ 0 & -2c_{0i} & -2c_{1i} & -2c_{2i} \\ 0 & 0 & -3c_{0i} & -3c_{1i} \end{bmatrix}, B_0 = \begin{bmatrix} 0 & 0 \\ 1 & -1 \\ 0 & 0 \\ 0 & 0 \end{bmatrix}, E_i = \begin{bmatrix} 0 \\ -c_{0i} \\ 0 \\ 0 \end{bmatrix}$$

$$B_u = \begin{bmatrix} 0 & 0 & 0 & 0 \\ 0 & 0 & 0 & 0 \\ 0 & 2 & 0 & 0 \\ 0 & 0 & 3 & 0 \end{bmatrix}, B_r = \begin{bmatrix} 0 & 0 & 0 & 0 \\ 0 & 0 & 0 & 0 \\ 0 & -2 & 0 & 0 \\ 0 & 0 & -3 & 0 \end{bmatrix}, F_{\mathrm{res},i}(z_i) = \begin{bmatrix} 0 \\ 0 \\ 0 \\ -3c_{2i}v_i^4 \end{bmatrix}$$

The reduced lifted system in (21) is further approximated by a first-order Taylor expansion around the current operating point $(\bar{z}_i(t), \bar{u}_i(t), \bar{r}_i(t))$, yielding an affine parameter-varying (APV) representation as:

$$\begin{aligned} \dot{z}_i(t) = \; & \tilde{A}_i(\bar{z}_i(t), \bar{u}_i(t), \bar{r}_i(t))\, z_i(t) + \\ & \tilde{B}_i(\bar{z}_i(t), \bar{u}_i(t), r_i(t))\, u_i(t) + \tilde{b}_i(\bar{z}_i(t), \bar{u}_i(t), r_i(t)). \end{aligned} \tag{22}$$

For implementation under the MPC framework, the APV lifted system (22) is discretized over one sampling interval Δt. By exact discretization of the frozen APV model within each sampling period, the discrete-time lifted predictor of train i is obtained as:

$$\begin{aligned} z_i(k+h+1|k) = \; & \bar{A}_i(k) z_i(k+h|k) \\ & + \bar{B}_i(k)\, u_i(k+h|k) + \bar{b}_i(k). \end{aligned} \tag{23}$$

The APV matrices are evaluated at the current state measurement $z_i(k|k)$, the most recent applied input $u_i(k-1)$ and the current exogenous input $r_i(k)$.

The order $\bar{n} = 3$ is used as the smallest truncation beyond the velocity-square observable required by the safety constraints, giving $z_i = [p_i, v_i, v_i^2, v_i^3]^\top$. Larger $\bar{n}$ may improve prediction accuracy but increases the lifted-state dimension and QP size. Thus, $\bar{n} = 3$ is a real-time-oriented design choice rather than a theoretically optimal order; a systematic sensitivity study is left for future work.

B. K-NMPC Formulation

Based on the lifted system, the nonlinear optimal control problem of each virtually coupled train can be reformulated as a Koopman-based NMPC problem in the lifted state space. For the leading train $i = 1$, the stage cost at time instant $k+h$ of sampling step k is defined as:

$$\theta_i^K(k+h|k) = \tag{24}$$

$$\begin{cases} \delta_{p,1}\big(z_{p,1}(k+h+1|k) - p_{\mathrm{ref}}(k+h+1)\big)^2 + \\ \quad +\delta_{v,1}\big(z_{v,1}(k+h+1|k) - v_{\mathrm{ref}}(k+h+1)\big)^2 \\ \quad +\delta_{u,1} u_1^2(k+h|k), \qquad i = 1 \\ \delta_{p,i}\big(z_{p,i-1}^*(k+h+1|k) - z_{p,i}(k+h+1|k) - \mathcal{D}_i\big)^2 \\ \quad +\delta_{v,i}\big(z_{v,i}(k+h+1|k) - z_{v,i-1}^*(k+h+1|k)\big)^2 \\ \quad +\delta_{u,i} u_i^2(k+h|k), \qquad i = 2, \dots, I \end{cases}$$

where $z_{p,i-1}^*(k+h+1|k)$ and $z_{v,i-1}^*(k+h+1|k)$ denote the predicted position and speed trajectories from train $i-1$.

At each sampling step k, the local KNMPC problem of train i is formulated as

$$\min\; J_i^K(k) = \sum\nolimits_{h=0}^{H_p} \theta_i^K(k+h|k) \tag{25}$$

$$\begin{aligned} \text{s.t.}\quad & z_i(k+h+1|k) = \bar{A}_i(k)\, z_i(k+h|k) + \\ & \qquad \bar{B}_i(k)\, u_i(k+h|k) + \bar{b}_i(k), \quad h = 0, \dots, H_p - 1, \\ & z_i(k|k) = \phi(x_i(k)), \\ & 0 \le z_{v,i}(k+h|k) \le v_i^{\max}(k+h|k), \quad h = 0, \dots, H_p, \\ & u_i^{\min} \le u_i(k+h|k) \le u_i^{\max}, \quad h = 0, \dots, H_p - 1, \\ & \Delta u_i^{\min} \le \frac{u_i(k+h+1|k) - u_i(k+h|k)}{\Delta t} \le \Delta u_i^{\max}, \\ & \qquad h = 0, \dots, H_p - 2, \\ & z_{p,i-1}^*(k+h|k) - z_{p,i}(k+h|k) - L_{i-1} \ge s_{m0}, \\ & \qquad h = 0, \dots, H_p, \quad \text{if } i = 2, \dots, I, \\ & z_{p,i-1}^*(k+h|k) - z_{p,i}(k+h|k) - L_{i-1} \\ & \quad \ge s_{m0} + \frac{z_{\sigma,i}(k+h|k)}{2b_{e,i}} - \frac{z_{\sigma,i-1}^*(k+h|k)}{2b_{e,i-1}}, \\ & \qquad h = 0, \dots, H_p, \quad \text{if } i = 2, \dots, I, \end{aligned}$$

where $z_{\sigma,i-1}^*(k+h|k)$ is the transmitted lifted observable corresponding to the squared speed of train $i-1$. The proposed KNMPC adopts the same distributed control framework based on information exchange between neighboring trains, as shown in Algorithm 1. The key difference lies in that each train solves the local lifted optimization problem (25), rather than the baseline NMPC problem.

V. Simulation Experiments

The simulations use realistic data from the 2265 m Tongji Nan–Jinhai Lu section of the Beijing Metro Yizhuang Line, with a 150 s scheduled trip. The leading-train reference (Fig. 2) is generated offline using GPOPS [27]. A two-train case is considered as a proof-of-concept scenario to evaluate the computational benefit of the Koopman-based local solver without cumulative communication delays from longer formations. The target spacing is $\mathcal{D}_i = 27$m, $H_p = 10$, $H_c = 1$, $\Delta t = 0.1$ s, and $\bar{n} = 3$. The weights are $\delta_{p,i} = 1$, $\delta_{v,i} = 5$, and $\delta_{u,i} = 0.001$. Simulations are performed in MATLAB R2020a on a PC with 16 GB RAM and a 2.4 GHz processor.

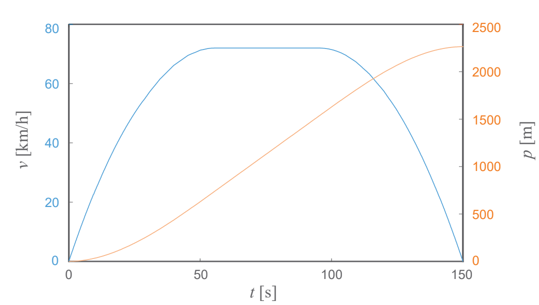

Fig. 2: Reference trajectory of the leading train.

TABLE II: Train Parameters (index i is dropped)

Symbol	*Value*	*Unit*
c_0	1.075×10^{-2}	N/kN
c_1	7.320×10^{-5}	$(\mathrm{kN} \cdot \mathrm{s})/(\mathrm{t} \cdot \mathrm{m})$
c_2	1.280×10^{-6}	$(\mathrm{kN} \cdot \mathrm{s}^2)/(\mathrm{t} \cdot \mathrm{m}^2)$
L	18.0	m
sm_0	4.0	m
d_{des}	9	m
b_e	1.2	$\mathrm{m/s^2}$
u^{min}	-1.10	kN/t
u^{max}	0.93	kN/t
$\Delta u^{min}/\Delta u^{max}$	-0.80/0.80	$\mathrm{m/s^3}$

A. Computational efficiency

The computational performance of D-KNMPC and D-BNMPC is evaluated across prediction horizons H_p ranging from 6 to 20. As illustrated in Fig. 3, D-KNMPC consistently achieves significantly lower computation times than D-BNMPC across all tested horizons. Specifically, the average computation time of D-KNMPC ranges from approximately 3.5 to 6.5 ms, with the maximum remaining below 15 ms. In contrast, D-BNMPC incurs substantially higher costs, with average computation times of 15 to 21 ms and maximum values exceeding 50 ms. These results indicate that D-KNMPC reduces computation time by approximately 65–70% relative to D-BNMPC while maintaining real-time feasibility, confirming its suitability for practical deployment.

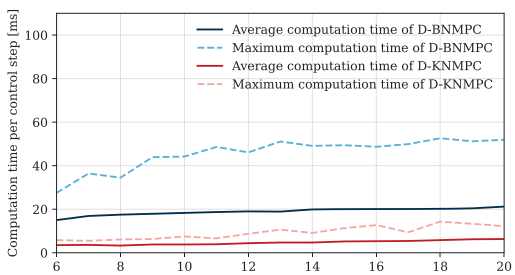

Fig. 3: Computation time for different predictive horizons

B. Control Performance Comparison

To further evaluate control performance, a comparative study between D-KNMPC and D-BNMPC is conducted. Fig. 4a presents the speed deviation profiles. The speed tracking performance of both methods is generally comparable, with identical mean absolute speed deviations of 0.006 m/s. However, D-KNMPC exhibits a larger transient deviation during the initial phase of Train 1, with the maximum absolute speed deviation increasing from 0.005 m/s under D-BNMPC to 0.303 m/s under D-KNMPC, attributable to the initial mismatch in the Koopman-lifted predictor. The spacing deviation profiles are shown in Fig. 4b. Both methods maintain small spacing deviations throughout most of the operation. However, D-BNMPC achieves tighter spacing tracking, with the maximum absolute spacing deviation being 0.213 m compared to 0.577 m under D-KNMPC. Additionally, D-KNMPC exhibits more pronounced spacing fluctuations in the later (decelerating) phase of operation.

The control input and control change rate profiles are illustrated in Fig. 5a and Fig. 5b, respectively. The overall

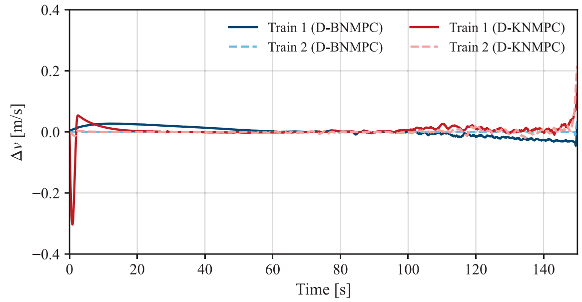

(a) Speed deviations.

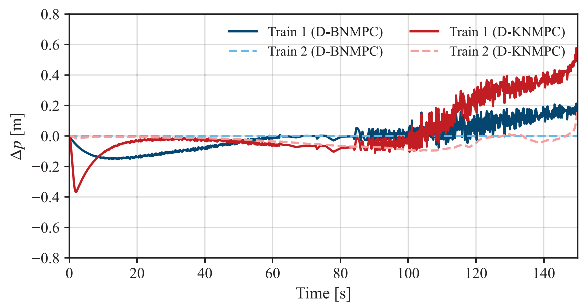

(b) Spacing deviations.

Fig. 4: Tracking performance.

control effort remains comparable between the two methods. Under both approaches, the control change rate stays within the prescribed bounds of $[-0.8, 0.8]$ m/s^3, confirming that the jerk constraints are strictly satisfied throughout the operation. Notably, D-KNMPC exhibits less fluctuation in the control change rate than D-BNMPC, indicating smoother control inputs and improved passenger comfort.

It should be noted that the considered scenario is a finite station-to-station operation rather than an infinite-horizon regulation task. The larger deviations observed near the terminal phase are mainly caused by the rapid deceleration of the reference trajectory and by the activation of input and input-rate constraints. During the simulated interval, the speed, control-force, control-rate, and collision-avoidance constraints remain satisfied. A formal closed-loop stability analysis of the distributed Koopman-based MPC scheme on infinite intervals is beyond the scope of this work and will be investigated in future research.

Since each train solves a local QP whose dimension depends only on the lifted state of a single train and the prediction horizon, the per-train computation cost is independent of the formation size I. The total time for the sequential solve scales linearly with I, remaining well within the sampling period for formations of practical size (e.g., three to five trains). The main scalability concern is the cumulative communication latency introduced by the sequential information propagation, which will be addressed in future work through delay-aware formulations.

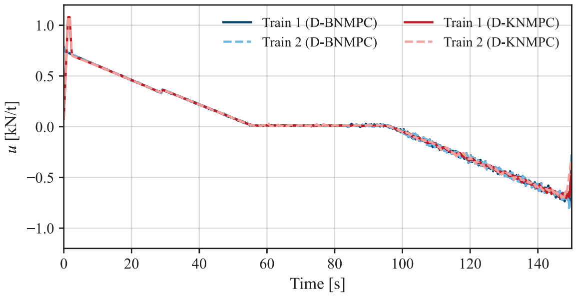

(a) Control forces.

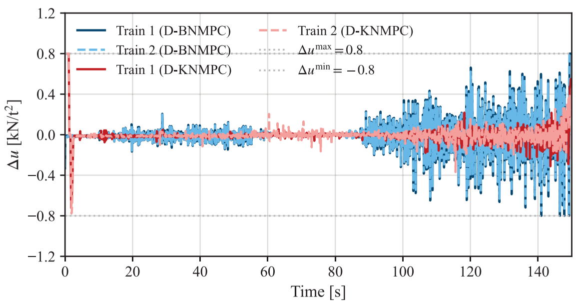

(b) Rates of change of control forces.

Fig. 5: Control inputs and rates of change.

VI. Conclusion

This paper presents a distributed Koopman-based NMPC framework for virtually coupled train control (VCTC) systems. Simulation results demonstrate that the proposed distributed KNMPC achieves tracking performance comparable to the baseline distributed NMPC while reducing average computation time by approximately 70%. Although larger transient deviations may appear during rapid acceleration or deceleration phases, all operational constraints remain satisfied in the tested finite-horizon scenario. These results confirm the effectiveness and real-time applicability of the proposed framework for VCTC systems. Future work will address delay-aware implementations for longer train formations and a systematic study of the truncation order $\bar{n}$, formal stability analysis, robustness against model uncertainties.

References

[1] I. Mitchell, E. Goddard, F. Montes, P. Stanley, R. Muttram, W. Coenraad, J. Poré, S. Andrews, and L. Lochman, "Ertms level 4, train convoys or virtual coupling," *IRSE NEWS*, vol. 219, pp. 1–3, 2016.

[2] T. Ständer, J. Drewes, I. Braun, and E. Schnieder, "Operational and safety concepts for railway operation with virtual train-sets," *IFAC Proceeding Volumes*, vol. 39, no. 12, pp. 261–266, 2006.

[3] M. Nold and F. Corman, "Train separation at cruising speed, how it can improve current railway operations," *Journal of Rail Transport Planning & Management*, vol. 30, p. 100451, June 2024.

[4] C. Di Meo, M. Di Vaio, F. Flammini, R. Nardone, S. Santini, and V. Vittorini, "Ertms/etcs virtual coupling: Proof of concept and numerical analysis," *IEEE Transactions on Intelligent Transportation Systems*, vol. 21, pp. 2545–2556, June 2020.

[5] D. Bauso, C. Fecarotti, and A. Khaleghi, "Cooperative control and stability analysis for virtual coupling of rail vehicles," *Control Engineering Practice*, vol. 133, p. 105452, 2023.

[6] Q. Zhang, H. Wang, Y. Zhang, and M. Chai, "An adaptive safety control approach for virtual coupling system with model parametric uncertainties," *Transportation Research Part C: Emerging Technologies*, vol. 154, p. 104235, 2023.

[7] E. Quaglietta, M. Wang, and R. M. Goverde, "A multi-state train-following model for the analysis of virtual coupling railway operations," *J. Rail Transp. Planning Manag.*, vol. 15, p. 100195, 2020.

[8] J. Xun, M. Chen, B. Ning, T. Tang, and H. Dong, "Train tracking performance measurement under virtual coupling in subway," *Journal of Beijing Jiaotong University*, vol. 43, pp. 96–103, February 2019.

[9] J. Felez and M. A. Vaquero-Serrano, "Virtual coupling in railways: A comprehensive review," *Machines*, vol. 11, no. 5, p. 521, 2023.

[10] G. Basile, D. G. Lui, A. Petrillo, and S. Santini, "Deep deterministic policy gradient virtual coupling control for the coordination and manoeuvring of heterogeneous uncertain nonlinear high-speed trains," *Engin. Appl. Artificial Intell.*, vol. 133, p. 108120, 2024.

[11] Y. Liu, Y. Zhou, S. Su, J. Xun, and T. Tang, "An analytical optimal control approach for virtually coupled high-speed trains with local and string stability," *Transportation Research Part C: Emerging Technologies*, vol. 125, p. 102886, April 2021.

[12] Y. Liu, R. Liu, S. Su, C. Wei, and T. Tang, "Distributed model predictive control strategy for constrained high-speed virtually coupled train set," *IEEE Trans. Vehicular Technol.*, vol. 71, pp. 171–183, 2022.

[13] X. Luo, T. Tang, J. Yin, and H. Liu, "A robust MPC approach with controller tuning for close following operation of virtually coupled train set," *Transp. Research Part C: Emerging Technologies*, vol. 151, p. 104116, 2023.

[14] X. Luo, T. Tang, X. Lu, J. Lv, and H. Liu, "Robust constraint satisfaction and stability of virtually coupled train set with uncertain dynamics: A dual-mode robust MPC approach," *Transp. Research Part C: Emerging Technologies*, vol. 156, p. 104356, 2023.

[15] J. Felez, Y. Kim, and F. Borrelli, "A model predictive control approach for virtual coupling in railways," *IEEE Transactions on Intelligent Transportation Systems*, vol. 20, pp. 2728–2739, July 2019.

[16] S. Su, J. She, K. Li, X. Wang, and Y. Zhou, "A nonlinear safety equilibrium spacing-based model predictive control for virtually coupled train set over gradient terrains," *IEEE Transactions on Transportation Electrification*, vol. 8, pp. 2810–2824, June 2022.

[17] D. Goswami and D. Paley, "Bilinearization, reachability, and optimal control of control-affine nonlinear systems: A Koopman spectral approach," *IEEE Trans. Autom. Control*, vol. 67, no. 6, pp. 2715–2728, 2021.

[18] M. Korda and I. Mezić, "Linear predictors for nonlinear dynamical systems: Koopman operator meets model predictive control," *Automatica*, vol. 93, pp. 149–160, 2018.

[19] L. Calogero, M. Boggio, C. Novara, and A. Rizzo, "A general analytical framework for fast solving nonlinear MPC problems in the linear Koopman space," in *Europ. Control Conf.*, pp. 743–748, 2025.

[20] P. Wang, J. Wang, Z. Li, T. Qu, F. Xu, Y. Hu, and H. Yang, "Koopman-MPC-based energy-efficient integrated control of attitude maneuver and vibration suppression for nonlinear in-wheel motor-active suspension on uneven roads," *Energy*, vol. 336, p. 138157, 2025.

[21] D. Gao, J. Peng, H. Peng, B. Chen, and Z. Huang, "Cooperative braking of urban rail vehicles with Koopman model predictive control," *IET Control Theory Appl.*, vol. 17, no. 15, pp. 2005–2016, 2023.

[22] H. Zheng, Y. Li, L. Zheng, and E. Hashemi, "Koopman-based hybrid modeling and zonotopic tube robust MPC for motion control of automated vehicles," *IEEE Transactions on Intelligent Transportation Systems*, vol. 25, no. 10, p. 13598, 2024.

[23] Y. Zhang, L. Calogero, S. Li, A. Rizzo, and A. Proskurnikov, "Koopman-based NMPC for virtually coupled train control system," *IFAC-PapersOnline*, 2026. to appear in IFAC World Congress 2026, available online.

[24] S. Iwnicki, M. Spiryagin, C. Cole, and T. McSweeney, *Handbook of Railway Vehicle Dynamics*. Boca Raton: CRC Press, 2nd ed., 2019.

[25] B. Tasseff, C. Coffrin, A. Wächter, and C. Laird, "Exploring benefits of linear solver parallelism on modern nonlinear optimization applications," 2019. online as arXiv 1909.08104.

[26] J. Andersson, J. Gillis, G. Horn, J. Rawlings, and M. Diehl, "CasADi: A software framework for nonlinear optimization and optimal control," *Math. Programm. Comput.*, vol. 11, no. 1, pp. 1–36, 2019.

[27] H. Ye and R. Liu, "A multiphase optimal control method for multi-train control and scheduling on railway lines," *Transportation Research Part B: Methodological*, vol. 93, pp. 377–393, 2016.